Supported Co–Re Bimetallic Catalysts with Different Structures as Efficient Catalysts for Hydrogenation of Citral — Source link ⧉

Xin Di, Xin Di, Gwendoline Lafaye, Catherine Especel ...+4 more authors

Institutions: Dalian University of Technology, University of Poitiers

Topics: Catalysis, Citral, Dehydrogenation and Bimetallic strip

Related papers:

- Influence of the nature of support on Ru-supported catalysts for selective hydrogenation of citral

- Mononuclear, Trinuclear, and Metallic Rhenium Catalysts Supported on MgO: Effects of Structure on Catalyst Performance.

- Catalytic hydrogenation of tertiary amides at low temperatures and pressures using bimetallic Pt/Re-based catalysts

- Selective Hydrogenation of Dimethyl Terephthalate to 1,4-Cyclohexane Dicarboxylate by Highly Dispersed Bimetallic Ru-Re/AC Catalysts.

- Adsorption, hydrogenation and dehydrogenation of C 2 H on a CoCu bimetallic layer

Supported Co-Re Bimetallic Catalysts with Different Structures as Efficient Catalysts for Hydrogenation of Citral

Xin Di, Gwendoline Lafaye, Catherine Especel, Florence Epron, Ji Qi, Chuang Li, Changhai Li

Supported Co-Re bimetallic catalysts with different structures as efficient catalysts for hydrogenation of citral

Xin Di [a], [b], Gwendoline Lafaye *[b], Catherine Especel [b], Florence Epron [b], Ji Qi [a], Chuang Li [a], Changhai Liang *[a]

[a] X. Di, J. Qi, C. Li, C. Liang, Laboratory of Advanced Materials and Catalytic Engineering, Dalian University of Technology, No.2 Linggong Road, Dalian City, Liaoning Province, P.R.China, E-mail: changhai@dlut.edu.cn

[b] G. Lafaye, C. Especel, F. Epron
Institut de Chimie des Milieux & Matériaux de Poitiers (IC2MP), Université de Poitiers, 4 rue Michel Brunet, 86073 Poitiers, France
E-mail: gwendoline.lafaye@univ-poitiers.fr

Abstract: Bimetallic Co-Re/TiO$_2$ catalysts were developed for efficient citral hydrogenation. Bimetallic catalysts were prepared by co-impregnation (CI), successive-impregnation (SI) and surface redox method (SR). The arrangement between Co and Re species on these systems was fully characterized by several techniques (TEM-EDX, H$_2$-TPR, TPD, XRD, CO-FTIR, model reaction of cyclohexane dehydrogenation) and their catalytic performances were evaluated for the selective hydrogenation of citral towards unsaturated alcohols. The Re and Co species are totally isolated in CI sample, presenting a very limited Co-Re interaction. In SI samples, metals coexist in a Janus-type structure with a concentration of Re around Co. Decoration/Core-shell structures are observed for SR samples resulting from the redox exchange between the metallic surface of the parent Co/TiO$_2$ catalyst and the Re^{7+} species of the modifier precursor salt. The contact degree between the two metals gradually increases as follows: Isolated structure (CI) < Janus-type structure (SI) < Decoration/Core-shell structure (SR). The unchanging structure of all SI samples whatever the Re loading leads to similar electron transfer and the increase in Re content results in agglomeration of rhenium, thus decreasing the catalytic activity. Density of state (DOS) calculation proves that high valence of Re is a disadvantage for hydrogenation reaction. For SR samples, the increase of Re loading contributes to the electron transfer from Re to Co, that is consistent with a change of structure from decoration to core-shell. The lack of directly accessible Co atoms for SR catalysts with fully coating structure decreases the reduction efficiency of Re. The presence of Co-Re interaction issued from close contact between metals plays a dominant role in the hydrogenation of citral. Nevertheless, excessive contact degree is unnecessary for citral hydrogenation once Co-Re interaction has formed.

Introduction

α, β-unsaturated aldehydes, such as citral, a naturally produced terpenoid abundantly found in the oil of lemon grass, can be selectively hydrogenated into unsaturated alcohols (UA), valuable intermediates widely used in perfumes, pharmaceuticals, pesticides and foods. Citral can be easily produced in large quantities without complicated synthesis steps, that makes the hydrogenation of citral an interesting economical route to obtain unsaturated alcohols [1]. Furthermore, this reaction is attractive to develop new catalytic formulations for application in the hydrogenation of bio-based molecules, since citral can be considered as a model molecule with three potentially hydrogenable double bonds, an isolated C=C bond in addition to conjugated C=C and C=O bonds, of which the selective hydrogenation is very sensitive to the nature and the arrangement of the active phases.

Noble metal-based monometallic catalysts are very active for C=C hydrogenation, but they frequently tend to exhibit over-hydrogenation activities associated with limited C=O hydrogenation properties [2]. Their modification by a non-noble promoter is a common way to increase their selectivity, and many bimetallic supported systems such as Pt-Ge, Pt-Co, Rh-Ge or Pd-Sn have demonstrated high catalytic performances for citral hydrogenation [3]. While rhenium can be an interesting promoter for this reaction, since it can effectively reduce C=O bond, to the best of our knowledge it has never been used as active phase for this reaction. As the activity of Re-based catalysts is significantly influenced by Re oxidation state, it is the most often associated with noble metals in bimetallic M-Re nanoparticles in order to improve catalytic activity [4].

In bimetallic catalysts, the first approach consists in the finding of optimal metal combination, but the different structures of the catalyst, and especially the contact degree between the two metals, can also play a crucial role in the synergetic effect [5]. For M-M' based bimetallic catalysts associating a metal M able to activate hydrogen to another one M' which is difficult to be reduce, the arrangement between the two metals can be roughly divided into two categories: (1) M is in close contact with M' and thus the dissociated hydrogen can directly transfer from M to M' [5a, 6], thus increasing the reduction efficiency of this latter. This direct bimetallic contact contributes to the possibility of geometrical effect and electron transfer between the two metal species; (2) M is isolated from M', and the dissociated hydrogen will transfer from M to M' via the support [5a, 6] and the possibility of electron transfer will be relatively limited. The type of contact between the two metals in bimetallic nanoparticles is complex, with the possible formation of alloy, core-shell or other shapes. Thus, more in tune with the reality, the reduction efficiency and electronic transfer will depend on the different structural properties. For example [5c], Pd(shell)–Au(core)/TiO$_2$, Au(shell)–Pd(core)/TiO$_2$ and PdAu(alloy)/TiO$_2$ catalysts were synthesized and the sample with Pd(shell) and Au(core) morphology exhibits higher activity for the total oxidation of VOCs than the other ones. Besides, some studies devoted to Pt-Co catalysts demonstrated that an intimate physical and/or chemical bimetallic interaction is not necessarily required to obtain a beneficial catalytic effect, since a simple mechanical mixture of Pt/Al$_2$O$_3$ and Co/Al$_2$O$_3$ was proven to improve the reducibility of Co$_3$O$_4$ species [5d]. It follows that the influence of different contact types on the structure and catalytic activity of nanoparticles depends strongly on the two metals and cannot be generalized.

Therefore, the purpose of this work was to investigate the influence of different types of contact in M-Re bimetallic catalysts on catalytic hydrogenation performances. With the aim of replacing costly and rare noble metals which are usually associated with Re [4a], this study will report the use for the first time of bimetallic Co-Re/TiO$_2$ catalysts for citral hydrogenation, with various degrees of metal-metal interactions depending on

the preparation method. Impregnation methods and a surface redox method [7] were chosen in order to prepare a series of Co-Re/TiO₂ samples with different contact degrees between the two metals.

Results and Discussion

Morphology and structure of CI and SI catalysts.

Firstly, the structures of the bimetallic Co-Re/TiO₂ samples prepared with CI and SI methods were analyzed. Figure 1(A)-(E) compares the TEM-EDX results obtained for both Re and Co monometallic samples and the SI and CI bimetallic catalysts. Figure 1(A) shows that 5Re/TiO₂ consists of very small particles (mean diameter = 0.8 nm) well-dispersed on the titania surface. The lattice spacing (2.10 Å) observed on HRTEM images clearly points to hexagonal rhenium [101] lattice plane. According to Figure 1(B), 5Co/TiO₂ catalyst shows a high dispersion of Co particles on TiO₂ although the particle size is rather big (~ 25 nm). The large accumulation of Co particles makes lattice spacing difficult to be observed by HRTEM in Figure 1(B).
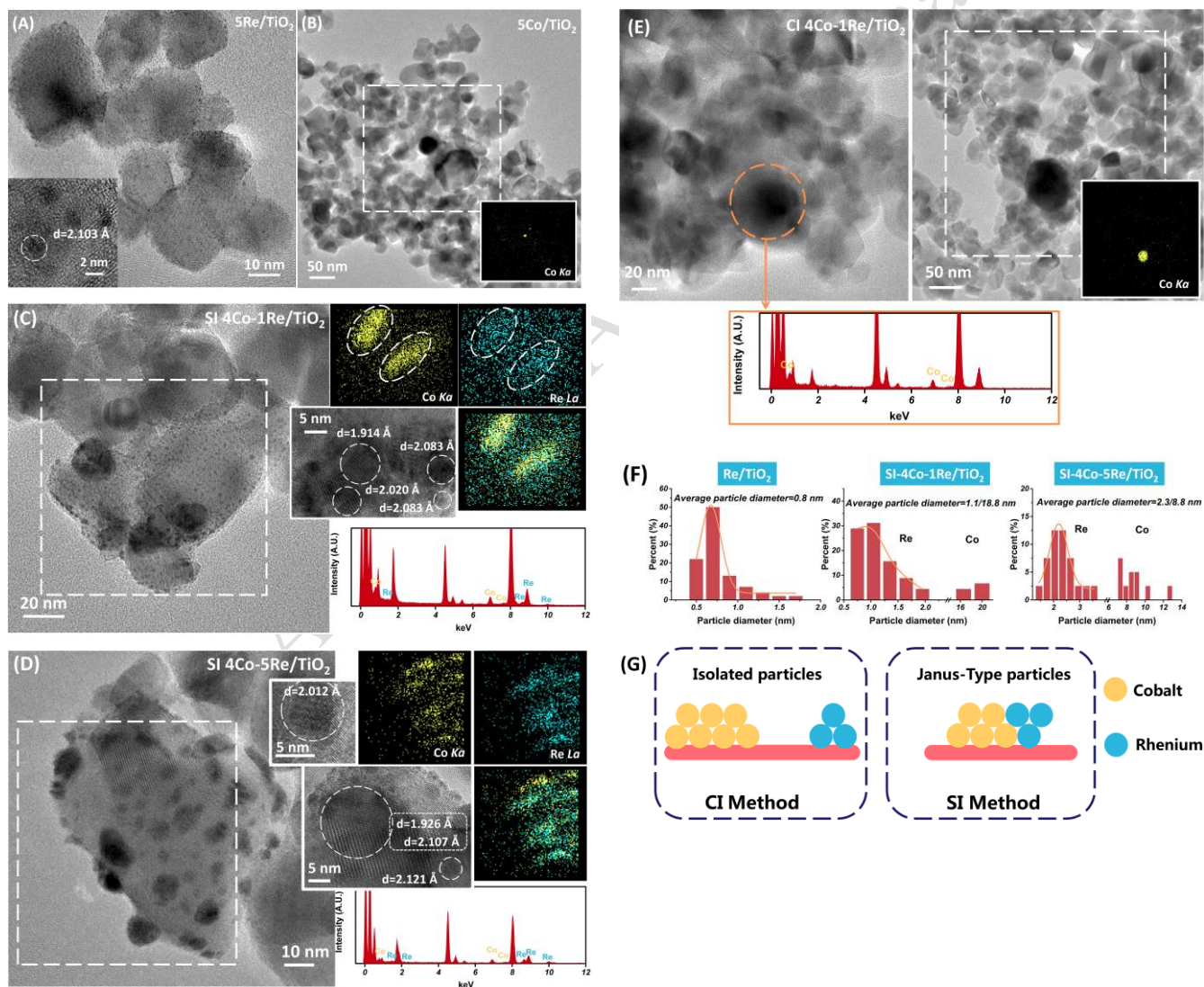

Figure 1. TEM-EDX and elemental mapping of (A) 5Re/TiO₂, (B) 5Co/TiO₂, (C) SI-4Co-1Re/TiO₂, (D) SI-4Co-5Re/TiO₂ and (E) CI-4Co-1Re/TiO₂. (F) Particle distribution of 5Re/TiO₂ and SI samples. (G) Schemes of CI and SI catalysts structure.

Figure. 1(C) and Figure. 1(D) show the TEM and corresponding elemental mapping for SI-4Co-1Re/TiO$_2$ and SI-4Co-5Re/TiO$_2$ samples, respectively. For SI-4Co-1Re/TiO$_2$, the lattice spacing 2.02 Å, 1.91 Å and 2.08 Å can be attributed to the Co [111], Co [101] and Re [101] lattice planes, respectively. Similar lattice spacing 2.01 Å, 1.93 Å and 2.11 Å assigned to Co [111], Co [101] and Re [101] lattice planes, respectively, were observed on SI-4Co-5Re/TiO$_2$. The little shift in lattice spacing compared with monometallic Re/TiO$_2$ is caused by the Co-Re interaction and the influence of the support. According to elemental mappings obtained on both SI samples, Re and Co do not exist as isolated species thus indicating the presence of bimetallic entities. Based on TEM results, Co-Re bimetallic catalysts prepared by SI method can be described mainly by a Janus-type structure (Figure 1(G)) with particles displaying two size populations as illustrated on Figure 1(F). Indeed, the metallic Co species pre-existing on the 5Co/TiO$_2$ catalyst can contribute to the reduction of NH$_4$ReO$_4$ precursor during the second impregnation step, which will be also in favor of concentrating Re particles around Co (these Re particles exhibit relatively small average sizes, *i.e.* 1.1 and 2.3 nm for SI-4Co-1Re/TiO$_2$ and SI-4Co-5Re/TiO$_2$ samples, respectively). Further, agglomeration of rhenium is gradually significant with the increasing of Re content according to average particle size. Besides, these Re species as deposited on the catalyst surface contribute to the re-dispersion of Co species in return, leading to a decrease of the particle size of cobalt. Indeed, when Re loading increases from 1 wt.% to 5 wt.% on the SI catalysts, the average particle size of Co decreases from 18.8 to 8.8 nm, which is in all cases lower than that observed for the Co/TiO$_2$ parent sample.

Concerning the CI-4Co-1Re/TiO$_2$ sample, rhenium particles are not found in Figure 1(E), which may be caused by the low loading and highly dispersion of Re. Furthermore, the average particle size of Co is similar to that of monometallic Co catalyst. It seems that Co and Re species exist as isolated monometallic particles and that there is almost no interaction between them in this sample (Figure 1(G)). The difference in structure between CI-4Co-1Re/TiO$_2$ and SI-4Co-1Re/TiO$_2$ catalysts can be explained by the different preparation methods used to synthesis these samples. Especially, in the case of SI sample, the Co species are pre-reduced before impregnation of Re salt what undeniably contributes to generate Co-Re interactions.

TPR analysis was used to characterize the reducibility of catalysts. This technique shows the way in which different species in the catalyst interact with each other. The results of the temperature programmed reduction experiments and the reduction degree of Re species are shown in Figure 2 for Co and Re monometallic samples, as well as for CI and SI bimetallic samples, all analyzed directly after the impregnation step of the Co and/or Re salts. The profile for the bare TiO$_2$ support presents a reduction peak at around 300 °C which originates from the surface reduction of TiO$_2$, however the resulting H$_2$ consumption is very small which could be ignored compared with the consumptions obtained on other samples.

The main reduction temperatures for 4CoCl$_2$/TiO$_2$ at 441 and 526 °C can be attributed to the gradual reduction of CoCl$_2$ precursor. The complete reduction of the Co^{2+} species of the CoCl$_2$/TiO$_2$ catalyst is obtained at the end of the TPR procedure according to the value of H$_2$ consumption. Besides, the TPR experiment performed on the *ex situ* reduced Co/TiO$_2$ monometallic catalyst (result not shown) leads to a very small H$_2$ consumption. This result reveals that the cobalt species are practically not oxidized during the storage of the catalyst. The reduced cobalt species are then stable on this sample. On the other hand, Figure 2 shows that monometallic Co/TiO$_2$ can be oxidized by water since the 4Co-H$_2$O/TiO$_2$ sample consumes an important amount of

hydrogen during TPR analysis. The reduced monometallic Co catalyst is thus oxidized after immersion in pure water [8], but the reduced state can be recovered by a subsequent reduction treatment.
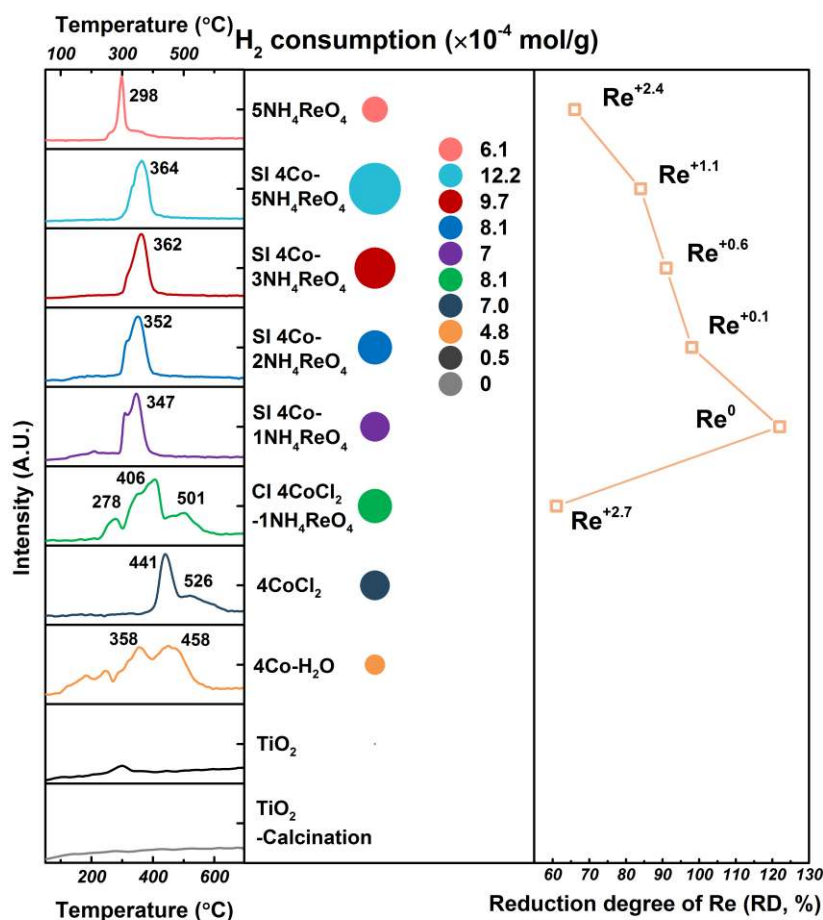

Figure 2. H_2-TPR results of SI-4Co-XNH$_4$ReO$_4$/TiO$_2$, CI-4CoCl$_2$-1NH$_4$ReO$_4$/TiO$_2$, 5NH$_4$ReO$_4$/TiO$_2$, 4CoCl$_2$/TiO$_2$, 4Co-H$_2$O/TiO$_2$ and bare TiO$_2$ support. In Re^n, n indicates the oxidation state at the end of the TPR. (4Co-H$_2$O/TiO$_2$: 4 wt.% Co/TiO$_2$ was *ex situ* reduced, treated by water for 12 h, then dried under 90 °C for 24 h after evaporation).

Since the reduction degree of Re could play a key role in the structure and performance of bimetallic catalysts, this one was determined from TPR results obtained for the SI and CI bimetallic catalysts according to the (1) and (2) following formulas:

(1) Reduction degree (RD %) of Re for SI-4Co-XNH$_4$ReO$_4$/TiO$_2$ catalysts

$$= \frac{\text{Hydrogen consumption of SI-4Co-XNH}_4\text{ReO}_4\text{/TiO}_2 - \text{Hydrogen consumption of 4Co-H}_2\text{O/TiO}_2}{\text{Expected hydrogen consumption of Re precursor for SI-4Co-XNH}_4\text{ReO}_4\text{/TiO}_2} \times 100$$

(2) Reduction degree (RD %) of Re for CI-4Co-1NH$_4$ReO$_4$/TiO$_2$

$$= \frac{\text{Hydrogen consumption of CI-4CoCl}_2\text{-1NH}_4\text{ReO}_4\text{/TiO}_2 - \text{Hydrogen consumption of 4CoCl}_2\text{/TiO}_2}{\text{Expected hydrogen consumption of Re precursor for CI-4CoCl}_2\text{-1NH}_4\text{ReO}_4\text{/TiO}_2} \times 100$$

(3) Average oxidation state of Re after reduction of the SI or CI sample = +[7 × (1 - RD(%) / 100)] with RD ≤ 100%

In each case, the expected hydrogen consumptions were calculated by assuming the fully reduction of Re^{7+} precursor. From the reduction degree values, an average valence state was then estimated for the Re species of each Re-based catalyst (equation (3)).

The TPR results of $5NH_4ReO_4/TiO_2$ sample show that Re precursor salt impregnated alone on the titania support cannot be fully reduced in the studied temperature range, and the hydrogen consumption value indicates that the Re species are stoichiometrically reduced until an average oxidation state of +2.4. So we can make the hypothesis that Re is mainly present as a mixture of Re^0 and high valence Re^{n+}, such as Re^{3+}, Re^{4+} and/or Re^{7+}. The reduction peak for bimetallic SI-4Co-XNH$_4$ReO$_4$/TiO$_2$ catalysts is located around 350 °C, *i.e.* between the temperature ranges observed on monometallic $5NH_4ReO_4/TiO_2$ sample (thin peak at 298 °C) and on the $4Co-H_2O/TiO_2$ sample (large massif until 500 °C). Therefore, this result can be attributed to the co-reduction of Re and Co species. The significantly higher reduction degree of Re for SI bimetallic catalysts compared to the monometallic Re sample signifies an improvement in the rhenium reducibility. The Co-Re interaction coming from Janus-type structure of SI bimetallic samples contributes to the reduction of NH_4ReO_4 precursor, which in turn is in favor of concentrating Re particles around Co. In that case, the reduction efficiency of Re should gradually decrease with increasing the Re loading, because of the agglomeration of rhenium clusters. The H_2-TPR results effectively prove this conclusion since the average oxidation state of Re after reduction increases from 0 to +1.1 with Re loading increasing from 1 wt.% to 5 wt.%. The SI-4Co-1NH$_4$ReO$_4$/TiO$_2$ catalyst exhibits even a value of reduction degree above 100 %, so a very superior reduction efficiency than other catalysts of the series. It also means that not only the surface redox process but also the hydrogen spillover is involved in the Re reduction mechanism, beneficial for Co-Re interaction. The H_2-TPR profile of CI-4CoCl$_2$-1NH$_4$ReO$_4$/TiO$_2$ catalyst can be understood as the addition of the profiles of $4CoCl_2/TiO_2$ and $5NH_4ReO_4/TiO_2$ monometallic samples. Although the reduction range of $CoCl_2$ species appears at slightly lower temperature on the CI bimetallic catalyst than on the monometallic $4CoCl_2/TiO_2$ sample, the reduction degree and average oxidation state of Re (+2.7) are comparable to the value obtained on monometallic $5NH_4ReO_4/TiO_2$ sample. This result demonstrates that a Co-Re interaction is not clearly present in CI-4Co-1Re/TiO$_2$ sample, as previously proved by TEM results. To achieve significantly improvement in Re reducibility, the intimate contact between Co and Re is then necessary in Co-Re bimetallic samples. The Re and Co isolated particles in CI sample are disadvantageous for increasing Re reduction efficiency compared with Janus-type structure in SI samples.

This series of catalysts was also characterized by H_2-TPR after their preparation and activation by reduction. For that purpose, the samples were pre-oxidized at 300 °C for 1 h prior to the TPR experiment. The results and specific analysis are shown in Supporting Information (Figure S1). It leads to a same conclusion as the one emerging from the discussion above proving the existence of a contact between Re and Co species in SI samples thus modifying their reduction properties.

Morphology and structure of SR catalysts.

The differences in metal arrangement and in Co-Re interactions observed between CI-4Co-1Re/TiO$_2$ and SI-4Co-1Re/TiO$_2$ catalysts result from the different methods used to prepare these samples. For SI samples, the Co species are pre-reduced before impregnation of Re salt. In that case, we can assume that a redox reaction occurs between the reduced Co species and the Re salt. To verify this hypothesis, a series of Co-Re bimetallic catalysts was prepared by enhancing the surface redox reaction between the pre-reduced parent Co and the oxidized form of Re. The preparation protocol is given in the catalyst preparation section and the resulting catalysts are referred as SR-*X*Co-*Y*Re/TiO$_2$ (*X* and *Y* represent the respective expected weight metal loadings).
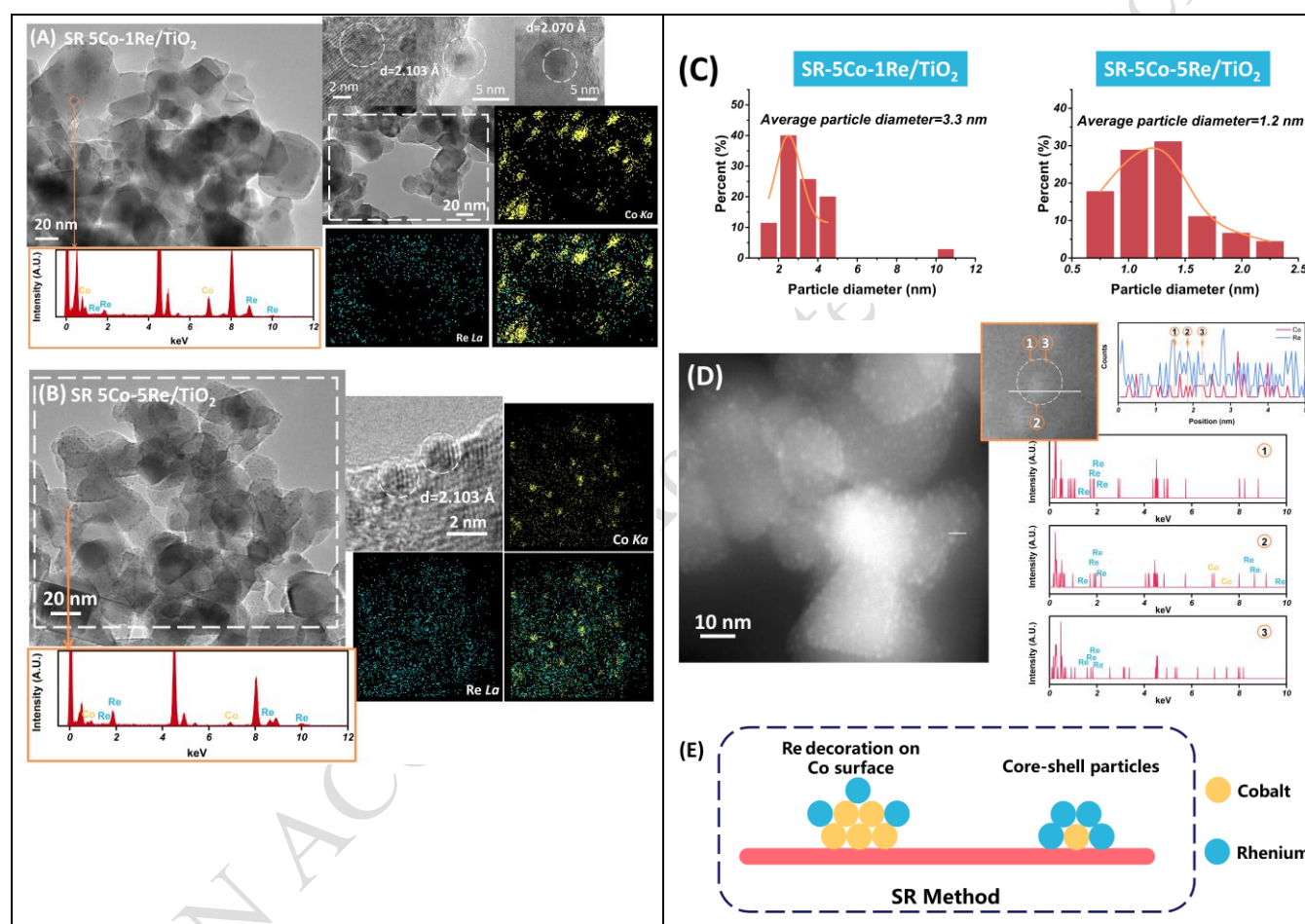
Figure 3. TEM-EDX and elemental mapping of (A) SR-5Co-1Re/TiO$_2$ and (B) SR-5Co-5Re/TiO$_2$. (C) Particles distribution of SR samples. (D) HAADF-STEM, linear scanning and associated EDX of SR-5Co-5Re/TiO$_2$. (E) Schemes of SR catalysts structure.

Figure 3(A) and Figure 3(B) illustrate the TEM-EDX results obtained for SR-5Co-1Re/TiO$_2$ and SR-5Co-5Re/TiO$_2$ catalysts prepared by surface redox reaction. The existence of a single population of particle size and the EDX analysis prove that Re is tightly bonded with Co generating bimetallic particles with quite homogeneous sizes. The elemental mappings show that the addition of Re induces a significant

decrease of the Co particle size, by comparison to the monometallic Co catalyst, which is in accordance with the preparation method principle. The decrease in average particle size intensifies with increasing Re loading, with average values evolving from 3.3 to 1.2 nm (Figure 3(C)). Moreover, the distribution of Re becomes much denser for SR-5Co-5Re/TiO$_2$ than that for SR-5Co-1Re/TiO$_2$ (Figure 3(B) compared to Figure 3(A)). These results suggest that the structure of SR catalysts gradually changes from decoration structure to core-shell structure when Re loading is high (Figure 3(E)). The SR preparation method, that is a redox process between Co metal and Re^{7+} ions of the Re precursor salt, can indeed promote the formation of such structures. For further insight into the structure of SR samples, SR-5Co-5Re/TiO$_2$ catalyst was analyzed by HAADF-STEM (Figure 3(D)). Unsurprisingly, the bimetallic particles are highly dispersed on TiO$_2$ support and the linear scanning of single particle exhibits that Co is fully covered by Re. Besides, the EDX results at different positions in linear scanning show that only Re is present on the edge of the observed particle (① and ③) and both Co and Re exist in the middle (②), which further confirms the core-shell structure of SR-5Co-5Re/TiO$_2$. This analysis was carried out on several randomly selected particles on SR-5Co-5Re/TiO$_2$ (Figure S2) leading to the same conclusion.

Figure S3 shows the H$_2$-TPR results of SR samples after their preparation, reduction and re-oxidation before TPR experiment. TPR profiles of SR-5Co-XRe/TiO$_2$ catalysts show that the addition of Re to Co/TiO$_2$ has a substantial effect on the reduction behavior: the reduction peaks of the SR bimetallic sample display a maximum around 320 °C $i.e.$ between the reduction ranges of both monometallic catalysts, and the bimetallic catalysts exhibit significantly higher hydrogen consumption ratios (HCR, Supporting Information) than monometallic catalysts, evidencing close contact between Re and Co species. An increase of Re content causes a decrease of the H$_2$/Re value and the SR-5Co-2Re/TiO$_2$ sample exhibits the highest HCR value of the SR bimetallic series. The SR method is based on the surface redox reaction between pre-existing Co metallic particles and Re oxidized species of the precursor salt, leading to decoration and core-shell structures. The deposition of a high Re content would protect Co surface of catalysts, leading to fully Re coated surface (Figure 3(E)). The lack of accessible Co atoms for SR-5Co-5Re/TiO$_2$ catalyst may limit the hydrogen transfer and then decrease the reduction efficiency of ReO$_x$ to a certain extent compared with other SR samples.

Further structural analysis of the different catalysts.
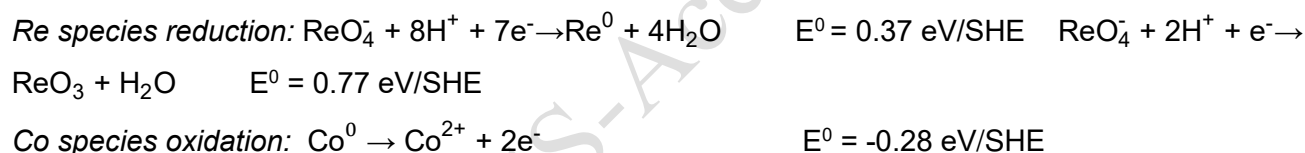
The catalysts prepared in this work present different metal arrangement and the contact degree between Co and Re would gradually increase in this order: CI sample (Isolated structure) < SI sample (Janus-type structure) < SR sample (Decoration and core-shell structures). In this part, the influence of catalyst structures on the interaction between metals will be analyzed and compared.

Table 1. Physicochemical properties of monometallic and bimetallic catalysts.

Samples /TiO$_2$	Metal loading (wt.%)		S$_{BET}$ (m^2 g^{-1})	V$_{pore}$ (cm^{-3} g^{-1})	Average pore size (nm)	Average particle size (nm) [a]	Acid sites (moL g^{-1}$_{cat}$) [b]
	Co	Re					
TiO$_2$	-	-	65.4	0.34	20.9	-	48
5Co	5.3	-	52.8	0.32	24.2	25	33
Cl-4Co-1Re	4.1	1.0	61.5	0.37	24.2	30	-
SI-4Co-1Re	4.2	1.0	55.6	0.38	27.2	1.1/18.8	33
SI-4Co-2Re	4.0	1.9	58.8	0.37	25.0	-	-
SI-4Co-3Re	4.0	2.8	53.7	0.34	25.0	-	-
SI-4Co-5Re	4.2	4.5	54.7	0.32	23.2	2.3/8.8	60
SR-5Co-1Re	4.0	1.1	58.6	0.34	23.1	3.3	40
SR-5Co-2Re	3.9	1.5	55.2	0.35	25.6	-	-
SR-5Co-5Re	2.2	4.8	51.8	0.31	23.9	1.2	68
5Re	-	4.5	66.1	0.33	19.7	0.8	42

[a] Determined by TEM analysis. [b] Determined by NH$_3$-TPD analysis.

The main characteristics of catalysts synthesized by different methods gathered in Table 1 show that the preparation of the Co-Re bimetallic catalysts results in a slight decrease in surface area of lone TiO_2, in a lower extend in the case of CI-4Co-1Re sample compared to the others. The pore volume and average pore size, around 0.35 cm^{-3} g^{-1} and 25 nm, respectively, are rather similar whatever the bimetallic sample. The ICP-OES analysis of the catalysts reveals that the actual metal loadings are in agreement with the expected ones. Moreover, it must be pointed out that for SR samples the Co content gradually decreases when increasing Re loading, because of the oxidation of Co metal atoms by Re ions and elimination of these oxidized species by filtration of the solution at the end of the SR protocol. A BLANK-5Co/TiO$_2$ sample was also prepared in order to evaluate the influence of the preparation conditions used during the SR preparation procedure on the monometallic Co/TiO$_2$ catalyst, and notably the acidity of the medium (pH 1). For that purpose, the parent 5Co catalyst was treated in the same way as for preparing a SR bimetallic catalyst but without introduction of the Re salt solution (replaced by a solution of water acidified to pH 1). Acid solution leads to a partial leaching of the Co phase since a decrease of the Co load is observed from 5.3 (5Co/TiO$_2$ sample) to 3.6 wt.% (BLANK-5Co/TiO$_2$). As the loss of Co content is lower on the SR-5Co-1Re and SR-5Co-2Re samples (Table 1), this suggests that during the SR procedure H$^+$ ions would be in priority involved in the reduction process of Re species instead of dissolving pre-existing Co atoms, according to the following possible surface redox reactions (E^0 values given for pH equal to 0):

Re species reduction: $ReO_4^- + 8H^+ + 7e^- \rightarrow Re^0 + 4H_2O$ \quad E^0 = 0.37 eV/SHE \quad $ReO_4^- + 2H^+ + e^- \rightarrow ReO_3 + H_2O$ \quad E^0 = 0.77 eV/SHE

Co species oxidation: $Co^0 \rightarrow Co^{2+} + 2e^-$ \quad E^0 = -0.28 eV/SHE
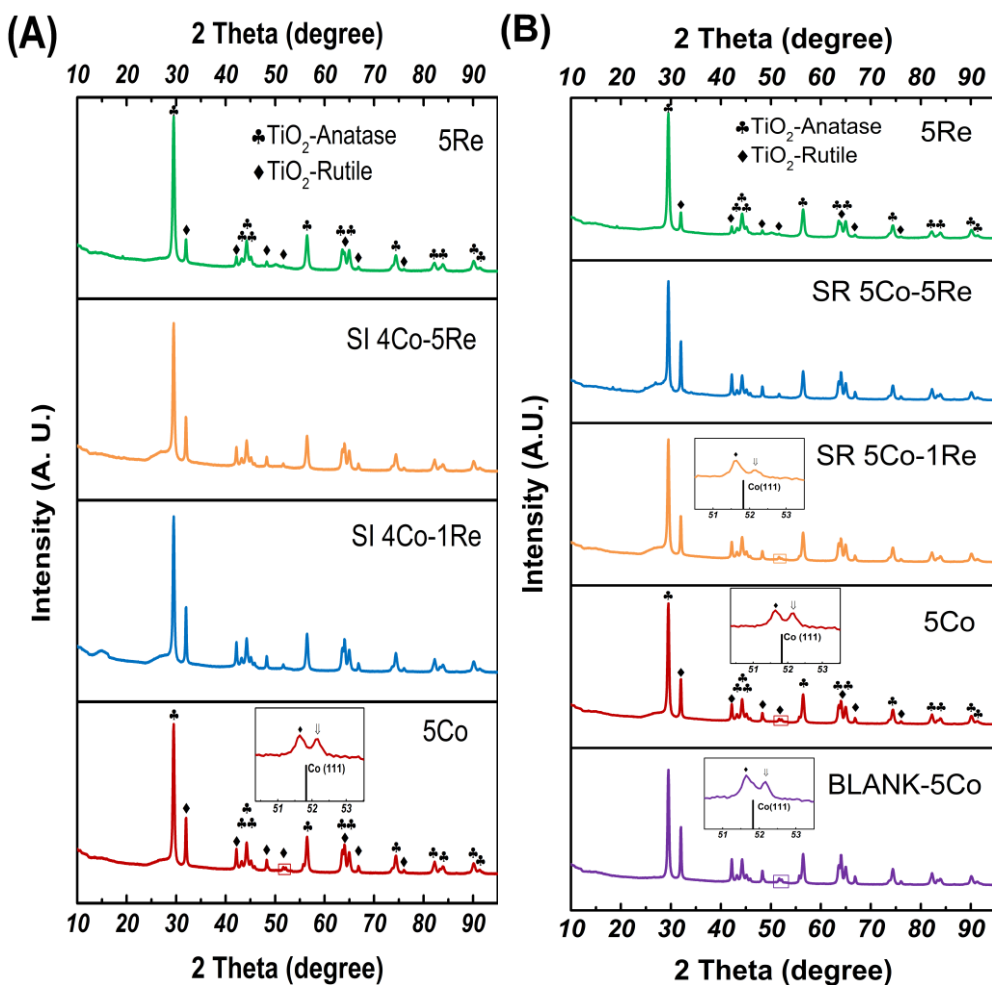
Figure 4. XRD patterns of Co-Re/TiO$_2$ catalysts prepared by SI (A) and SR (B) methods. BLANK-5Co/TiO$_2$: 5 wt.%Co/TiO$_2$ treated by HCl solution (pH 1) under N$_2$ atmosphere.

The XRD patterns of Co and Re monometallic catalysts, and of SI and SR bimetallic samples gathered in Figure 4, exhibit mainly peaks attributed to the TiO$_2$ support phases (anatase and rutile). No significant peak attributed to Re phase is observed for monometallic and bimetallic catalysts. It indicates that Re particles are very small or highly dispersed on TiO$_2$ support. A very small diffraction peak is observed on monometallic Co catalysts (zoom in the spectrum of the 5Co and Blank-5Co samples), however its position shifts a little compared with the value expected for any Co lattice plane. This shift may be explained by a lattice contraction of Co influenced by TiO$_2$ [9]. It is noteworthy that the XRD pattern of SR-5Co-1Re/TiO$_2$ catalyst also shows a very small diffraction peak. It implies that a small quantity of isolated Co species exists in this sample. Although Co species can be also observed on SI samples by TEM, a crystalline phase associated to totally isolated Co does not exist as the results of the influence of Janus-type structure.
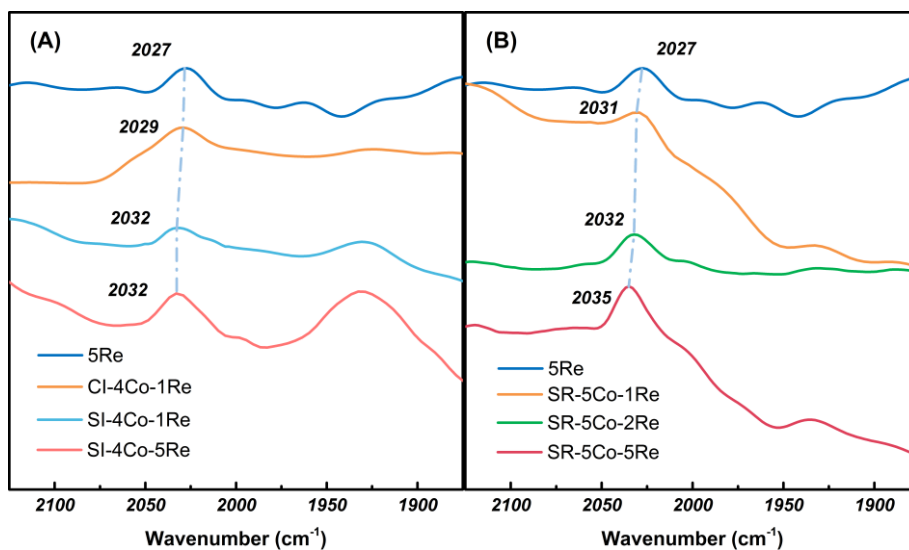
Figure 5. Infrared spectra of the adsorbed CO species over Re and Co-Re catalysts prepared by (A) CI, SI and (B) SR methods.

Figure 5 shows the *in situ* IR spectra of CO species adsorbed on monometallic Re and bimetallic Co-Re catalysts. CO adsorption on Co/TiO_2 results in a spectrum without any peak in the range 1850-2150 cm^{-1} (not shown). The spectrum of CO adsorbed on Re/TiO_2 reveals a band at 2027 cm^{-1}, assigned to linearly adsorbed CO on Re [10]. Linearly adsorbed CO was observed at 2032 cm^{-1} in the case of $SI-4Co-1Re/TiO_2$ and $SI-4Co-5Re/TiO_2$ catalysts that is at higher wavenumber compared to Re/TiO_2 (Figure 5(A)). This shift towards higher wavenumber indicates an electron transfer from Re to Co caused by Co-Re interaction [10-11]. Additionally, the v_{CO} value is the same for $SI-4Co-1Re/TiO_2$ and $SI-4Co-5Re/TiO_2$, implying similar structure for the various SI samples, which is consistent with TEM images indicating a Janus-type structure for all $SI-4Co-XRe/TiO_2$ catalysts. Besides, the wavenumber of CO adsorption peak for $CI-4Co-1Re/TiO_2$ is much closer to that obtained for the monometallic Re/TiO_2 proving the structure of isolated particles on that catalyst and limited Co-Re interaction. Figure 5(B) represents the FT-IR spectra of SR samples. The shift towards higher wavenumber for v_{CO} band is also observed for these samples, and moreover the wavenumber gradually increases from 2031 to 2035 cm^{-1} with the increasing of Re content. The different frequencies indicate the presence of different adsorption sites, that is, CO is adsorbed on Re atoms with different electron density. The arrangement of the metallic particles changes from decoration to core-shell structure for SR catalysts with the increasing of Re content, resulting in more significantly electron transfer. On the basis of these results, $SR-5Co-5Re/TiO_2$ sample shows a stronger Co-Re interaction than the $SR-5Co-1Re/TiO_2$ and $SR-5Co-2Re/TiO_2$ catalysts. To conclude, FT-IR analyses give clear evidence about the difference of structure and adsorption sites for Co-Re catalysts according to the preparation method. It also indicates that Re species in a metallic state are present on the samples after a reduction at 350 °C.
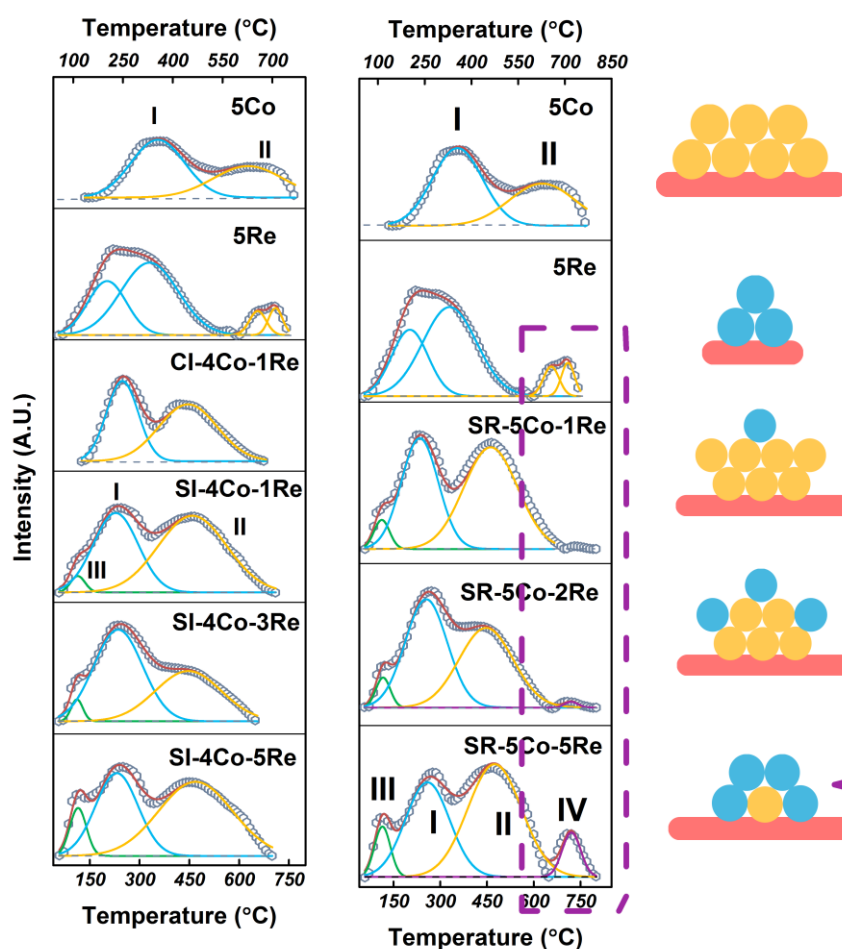
Figure 6. H$_2$-TPD profiles of monometallic Co, Re and bimetallic Co-Re samples.

A H$_2$-TPD analysis was also performed in order to study the hydrogen adsorption ability of the different samples and to relate the information to their structures (Figure 6 and Table 2). After being activated by metal, the adsorbed hydrogen can dissociate from catalysts in the course of the TPD analysis program. The hydrogen desorption amount of 5Co/TiO$_2$ catalyst was used as standard for quantitative analysis and the relative amount of hydrogen desorption was calculated with the following equation:

(4) Relative amount of hydrogen desorption

$$= \frac{\text{Peak area of 5Co, 5Re, SI-4Co-}X\text{Re or SR-5Co-}X\text{Re}}{\text{Peak area of 5Co}}$$

The hydrogen adsorption ability per mole of metal (APM) was calculated by defining the values corresponding to monometallic samples as equal to one, in order to evaluate the influence of Co-Re interaction on the hydrogen adsorption ability. The APM value was calculated according to the following equation:

(5) Hydrogen adsorption ability per mole of metal (APM) of bimetallic A sample

$$= \frac{\text{Peak area of A sample}}{\dfrac{\text{Co content of A sample}}{\text{Co content of 5Co}} \times \text{Peak area of 5Co} + \dfrac{\text{Re content of A sample}}{\text{Re content of 5Re}} \times \text{Peak area of 5Re}}$$

with A = CI-4Co-1Re, SI-4Co-XRe or SR-5Co-XRe catalyst

Table 2. H_2-TPD analysis of monometallic Co, Re and bimetallic Co-Re samples.

Samples/TiO$_2$	Relative desorption quantity	Hydrogen adsorption ability per mole of metal (APM)
5Co	1.00	1.0
5Re	1.54	1.0
CI-4Co-1Re	1.26	1.1
SI-4Co-1Re	1.94	1.7
SI-4Co-3Re	2.76	1.6
SI-4Co-5Re	2.86	1.2
SR-5Co-1Re	1.58	1.4
SR-5Co-2Re	2.40	1.9
SR-5Co-5Re	2.92	1.4

The thermal desorption curves of hydrogen for monometallic samples can be divided into two main peaks. Peak I ranging from 100 to 500 °C can be attributed to desorption of atomic hydrogen directly bonded to active metal Co and Re. The hydrogen adsorbed on the metal surface can migrate in the form of atomic hydrogen onto the neighboring support via surface diffusion, and the migrated atomic hydrogen desorbed at higher temperature (Peak II) [6a, 12]. The Co-Re interaction on SI samples results in the advanced desorption of a small amount of dissociated hydrogen at relative low temperature (Peak III) by weakening

the connection between atomic hydrogen and active metal. Further, the Co-Re interaction has also a positive influence on the hydrogen adsorption ability considering that the APM value of SI samples is significantly higher than monometallic and CI samples. As already discussed in H_2-TPR section, the Co-Re interaction would increase the reduction efficiency of Re which is then beneficial to hydrogen adsorption. The increase of Re content on SI samples leads to the agglomeration of particles and reduces the hydrogen adsorptio ability, manifesting as the gradually decrease of APM value with the increasing of Re loading for SI-4Co-XRe/TiO$_2$ catalysts.

By comparison with their SI counterparts, the SR-5Co-XRe/TiO$_2$ catalysts (with X = 2 and 5) exhibit superior hydrogen adsorption ability, especially for SR-5Co-2Re/TiO$_2$ sample displaying the highest APM value of the series (1.9), which is consistent with H_2-TPR results. Besides, the Co-Re interaction on SR catalysts also contributes to hydrogen desorption at lower temperature (Peak III). It is noteworthy that dissociated hydrogen on SR samples desorbed at around 700 °C (Peak IV) in a similar way than on 5Re/TiO$_2$ (Peak II). It indicates the existence of similar desorption sites, causing the consistent desorption behavior. The morphology of the SR catalysts changes from decoration to core-shell structure when increasing Re content, leading to the increase of Re coverage. The full coverage of Co by Re on SR-5Co-5Re/TiO$_2$ catalyst results in similar desorption behavior than that of monometallic Re/TiO$_2$. The results of H_2-TPD in turn prove the different structures of SR samples depending on the Re loading.

Catalytic results.

Dehydrogenation of cyclohexane to benzene was used as a probe reaction to evaluate the accessibility and the nature of active surface metal sites as this model reaction performed in gas phase is considered as structure insensitive. The results of cyclohexane dehydrogenation (Table 3) show that the total conversion obtained with SI bimetallic catalysts is higher than the one obtained on monometallic Co and Re catalysts and the value tends to increase with the increase of Re content. The monometallic Re/TiO$_2$ exhibits a low conversion, with similar percentages of dehydrogenated product (benzene) and by-products resulting from C-C cleavages (C1-C5 products). In addition, the percentage of by-products also gradually becomes majority for SI bimetallic catalysts when increasing Re loading. According to NH$_3$-TPD results (Table 1), the amount of acid sites is very small and comparable on all studied catalysts indicating that the C-C cleavages don't originate from cracking process on acid sites but rather from hydrogenolysis on metallic sites. It suggests that the presence of reduced Re species on SI samples caused by Co-Re interaction contributes to the hydrogenolysis of cyclohexane to C1-C5 products. The low conversion obtained for monometallic Re catalyst can be related to the high oxidation state of Re on this sample, which is not favorable neither for the dehydrogenation nor for the hydrogenolysis of cyclohexane. Thus, it indicates that the nature of the active surface of these catalysts is in accordance with the results obtained by TEM and H_2-TPR. In addition, the conversion to by-products with the CI-

4Co-1Re/TiO$_2$ catalyst, which exhibits a low Re reduction efficiency, is lower than that of SI-4Co-1Re/TiO$_2$.

Table 3. Catalytic performances for cyclohexane dehydrogenation and citral hydrogenation of monometallic Co, Re and bimetallic SI-4Co-XRe/TiO$_2$ and CI-4Co-1Re/TiO$_2$ catalysts.

Samples/TiO$_2$	Cyclohexane dehydrogenation [a]			Citral hydrogenation [b]		
	Total conversion (%)	Benzene (%)	By-products (%) [c]	Conversion at 30 min (%)	UA selectivity (%) [d]	Maximum UA yield (%) [e]
TiO$_2$	-	-	-	9.5	18.0	9.5
5Co	2.5	1.6	0.9	9.0	28.0	5.5
SI-4Co-0.5Re	4.6	2.8	1.8	46.0	41.5	47.0
SI-4Co-1Re	5.2	3.4	1.8	72.0	45.0	44.0
SI-4Co-2Re	7.3	4.4	2.9	57.0	46.4	48.0
SI-4Co-3Re	7.9	4.0	3.9	93.0	46.1	38.0
SI-4Co-5Re	8.9	3.9	5.0	99.3	45.0	40.0
CI-4Co-1Re	3.8	3.0	0.8	13.8	42.0	19.0
4Co + 1Re	1.1	0.9	0.2	8.8	37.2	12.1
5Re	0.4	0.2	0.2	22.0	20.0	12.2

[a] Reaction conditions: 300 °C, 80 mg catalyst, 100 mL min^{-1} H$_2$, 0.03 mL min^{-1} cyclohexane. [b] Reaction conditions: 70 °C, 0.4 g catalyst, 100 mL solution (3 mL citral), 75 bar H$_2$. [c] By-products: C1-C5 products issued from hydrogenolysis reactions. [d] UA selectivity determined at 40 % conversion. [e] Maximum yield reached during the 180 min reaction time.

The product distribution of citral hydrogenation over SI series samples is summarized in Figure 7 and Table 3. The hydrogenation of citral, an unsaturated aldehyde, is a consecutive reaction. Figure 7(A) summarizes the main reaction pathways that can occur during citral hydrogenation. The observed

products are (i) unsaturated products, *i.e.* citronellol, citronellal, nerol and geraniol (UA: unsaturated alcohols), and (ii) the saturated product 3,7-dimethyloctanol.
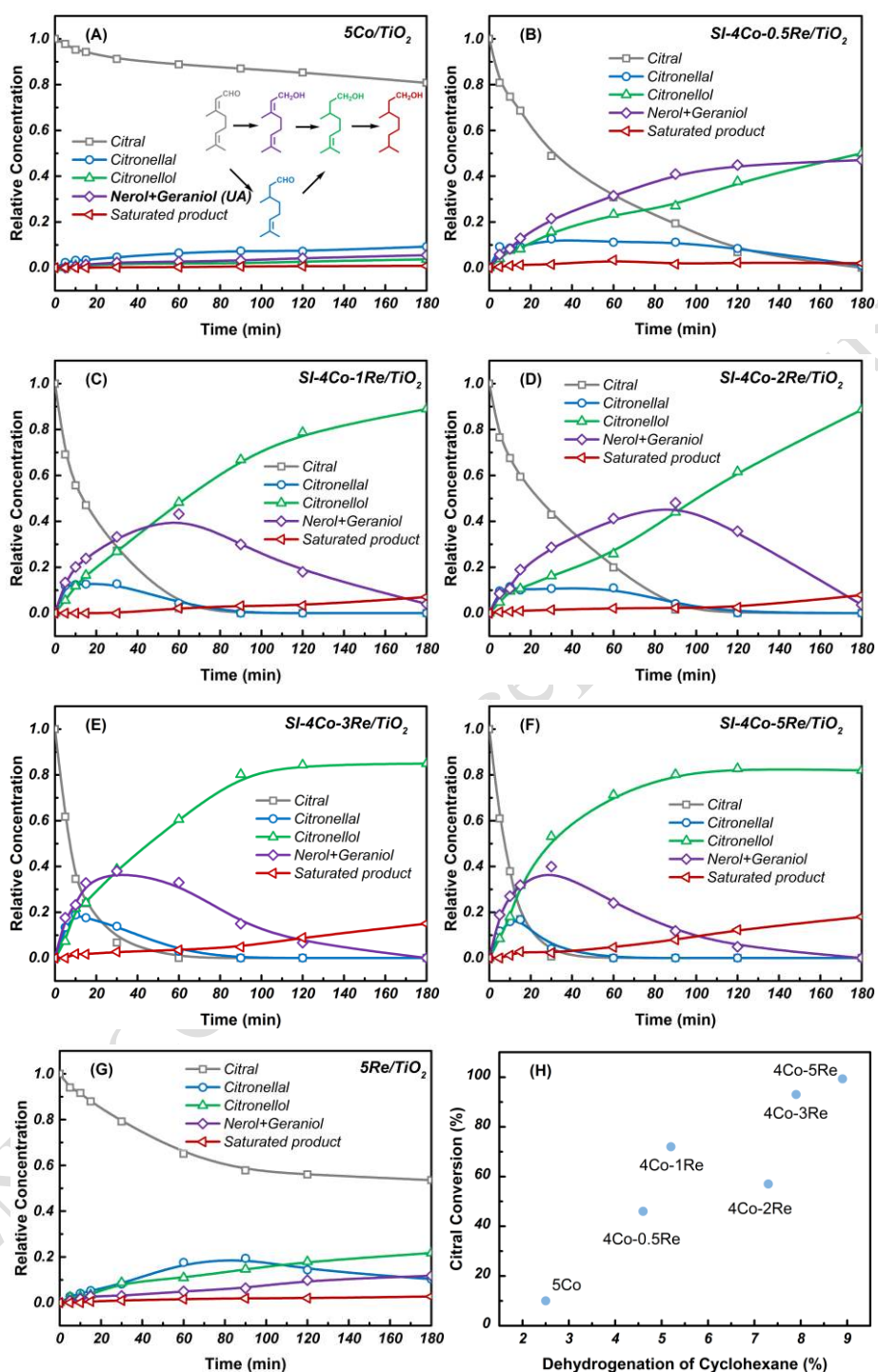

Figure 7. Citral hydrogenation on monometallic Co, Re and SI bimetallic catalysts. (Reaction conditions: 70 °C, 0.4 g catalyst, 100 mL solution (3 mL citral), 75 bar H_2)
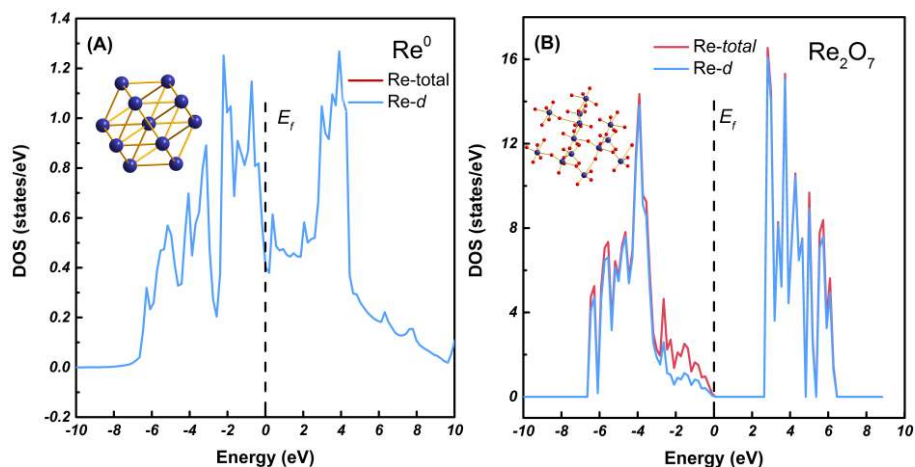
Figure 8. Total density of states (TDOS) and partial density of states (*d*-PDOS) of Re (A) and Re_2O_7 (B).

According to the results reported in Table 3, SI bimetallic catalysts exhibit significantly higher activity than monometallic Co and Re catalysts. For example, the conversion of citral after 30 min reaction time is 72 % for SI-4Co-1Re/TiO_2, largely higher than those of 5Co/TiO_2 (9 %) and 5Re/TiO_2 (22 %) under same reaction conditions. The citral conversion tends to increase with the Re content introduced, as previously observed for the cyclohexane dehydrogenation model reaction (Figure 7(H)). This confirms that the presence of accessible active sites increases with the addition of Re by SI method. This synergetic effect on activity for citral hydrogenation observed for SI samples can result from the influence of Co-Re interaction on the reaction and in particular from the changes in the oxidation state of the active species. The Janus-type structure of SI catalysts can contribute to the reduction of Re species, increasing consequently the activity. In order to further investigate this effect, we calculated the total density of states (TDOS) and partial density of states related to *d*-state (*d*-PDOS) of a surface constituted of Re^0 or Re_2O_7 atoms, corresponding to the extreme valence states of Re species participating in the adsorption process during the catalytic reaction. The results in Figure 8 show that the adsorption capacity and thus catalytic activity of Re-based components are decided by *d*-state of Re element, because it makes major contribution to TDOS. As far as we know, the TDOS and *d*-PDOS at Fermi level (E_F) would influence the adsorption and activation of active components on active metal [13]. Re^0 exhibits higher DOS at E_F compared with Re_2O_7 for which states density is zero, demonstrating that catalytic activity of Re_2O_7 is weakened by the presence of oxygen. The significant band gap nearby E_F for Re_2O_7 is disadvantage for citral hydrogenation reaction when it is regarded as main active sites. It further proves the attenuation of catalytic activity for catalysts with high valence Re element. Besides, the lack of electron density of Re^0 shown previously by FT-IR of adsorbed CO on SI samples may be beneficial to the adsorption of electron rich oxygen of aldehyde functions, which would also enhance the activity.

Although SI bimetallic samples with high Re loadings (3 and 5 wt.%) show superior conversion, the efficiency of active metals calculated by taking into account the actual total metal loadings seems quite comparable with that of the SI-4Co-1Re catalyst, less loaded in Re (Figure 9(A)). Moreover, when

considering Re as major contributor in the transformation of citral (Figure 9(B)), the SI-4Co-1Re sample finally appears as the most efficient of the SI catalyst series. The progressive decrease in the efficiency of SI-4Co-XRe catalysts as function of the increasing Re content can be attributed to the partial agglomeration and lower reduction of Re particles.
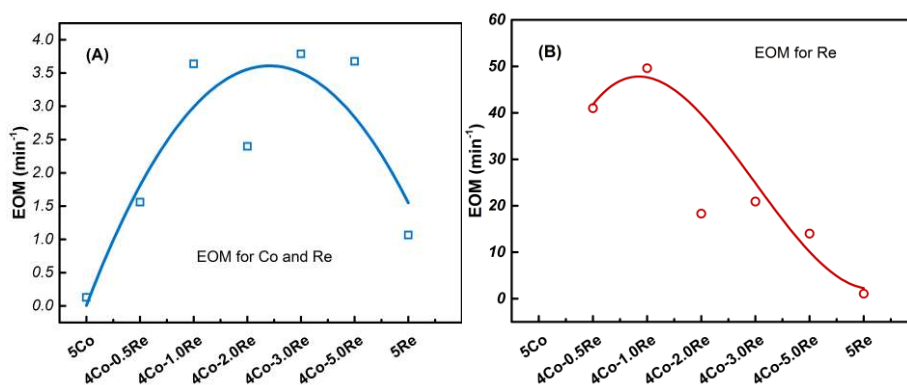

Figure 9. The efficiency of metal (EOM) for hydrogenation of citral on SI bimetallic catalysts series.

Concerning the products distribution obtained during citral hydrogenation, a similar selectivity to UA, around 45% for a 40% conversion, is observed for all SI bimetallic catalysts, which is consistent with the presence of the same Janus-type structure and the same nature of active sites for all these systems.

The influence of the Co-Re bimetallic interaction on catalytic performances can be evaluated by comparing the 4Co-1Re/TiO$_2$ systems prepared either by successive (SI) or co-impregnation (CI), or by a physical mixture of 4Co/TiO$_2$ and 1Re/TiO$_2$ catalysts (Table 3). The CI-4Co-1Re/TiO$_2$ sample displays poor performances for the citral hydrogenation and cyclohexane dehydrogenation, resulting from the presence of isolated Co and Re entities and the absence of Co-Re interaction. During the preparation of this sample, the absence of Co^0 species at the surface of the catalyst prevents the deposition of Re precursors in contact with Co particles and thus the formation of Co-Re interaction favoring the reduction of Re species. The physical mixture of 4Co/TiO$_2$ and 1Re/TiO$_2$ catalysts exhibits even lower activities, demonstrating that close contact between the metals is necessary to achieve a catalytic promotion effect. Therefore, the SR catalysts with higher contact degree between metals than SI samples were evaluated for the hydrogenation of citral.

Table 4 compares the catalytic results of cyclohexane dehydrogenation and citral hydrogenation obtained with the SR bimetallic series to those displayed by the Co and Re monometallic samples. The lower activity in cyclohexane dehydrogenation of BLANK-5Co/TiO$_2$ compared to the parent 5Co/TiO$_2$ results from the decrease of active sites caused by acid treatment (partial loss of Co by leaching as observed by ICP-OES, from 5.3 wt.% to 3.6 wt.%).

Table 4. Catalytic performances for cyclohexane dehydrogenation and citral hydrogenation of monometallic Co, Re and bimetallic SR-5Co-XRe/TiO_2 catalysts.

Samples/TiO_2	Cyclohexane dehydrogenation [a]			Citral hydrogenation [b]		
	Total conversion (%)	Benzene (%)	By-products (%) [c]	Conversion at 30 min (%)	UA selectivity (%) [d]	Maximum UA yield (%) [e]
5Co	2.5	1.6	0.9	9.0	28.0	5.5
BLANK-5Co [f]	1.3	0.8	0.5	11.4	35.1	7.9
SR-5Co-1Re	4.4	3.4	1.0	20.1	48.0	12.1
SR-5Co-2Re	5.0	3.6	1.4	77.8	43.4	44.6
SR-5Co-5Re	8.4	3.8	4.6	98.0	52.0	51.0
5Re	0.4	0.2	0.2	22.0	20.0	12.2

[a] Reaction conditions: 300 °C, 80 mg catalyst, 100 mL min^{-1} H_2, 0.03 mL min^{-1} cyclohexane. [b] Reaction conditions: 70 °C, 0.4 g catalyst, 100 mL solution (3 mL citral), 75 bar H_2. [c] By-products: C1-C5 products issued from hydrogenolysis reactions. [d] UA selectivity determined at 40 % conversion. [e] Maximum yield reached during the 180 min reaction time. [f] BLANK-5Co/TiO_2: 5 wt.%Co/TiO_2 treated by HCl solution (pH 1) under N_2 atmosphere
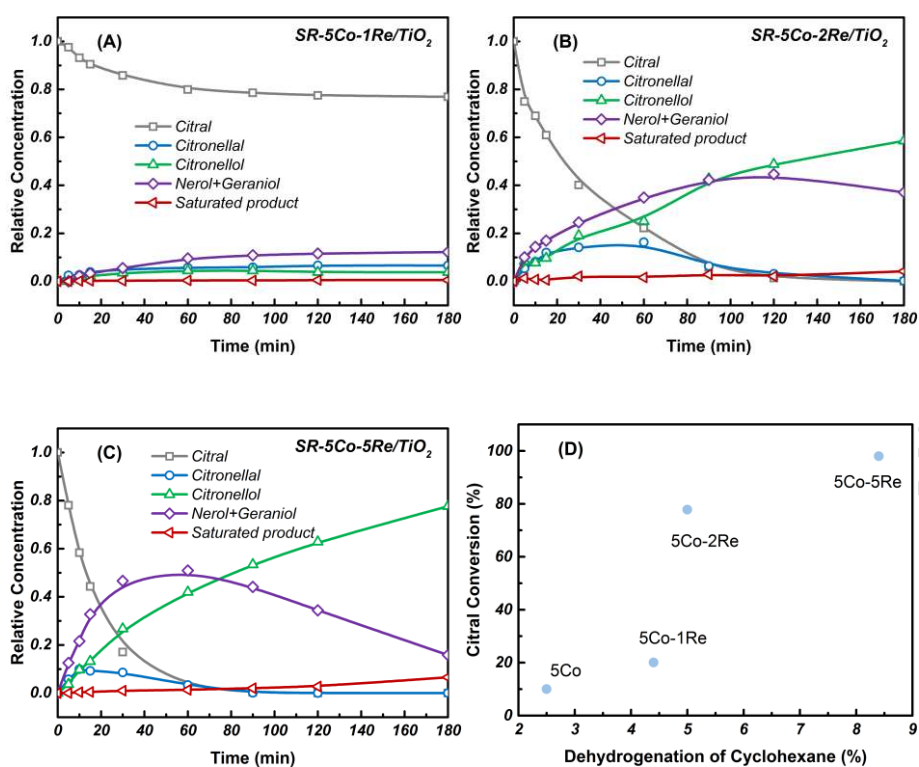
Figure 10. Citral hydrogenation on SR bimetallic catalysts. (Reaction conditions: 70 °C, 0.4 g catalyst, 100 mL solution (3 mL citral), 75 bar H_2)

As with the SI bimetallic series, the percentage of by-products formed during the cyclohexane dehydrogenation also gradually becomes predominant for SR bimetallic catalysts when increasing Re loading. In the same way as in the SI catalysts, the reduced Re species in SR samples play an important role in the production of these C1-C5 products. Especially for SR-5Co-5Re/TiO2 with a core(Co)-shell(Re) structure exhibits highest selectivity to C1-C5 products, which confirm the influence of reduced Re on cyclohexane dehydrogenation. Furthermore, the SR catalysts exhibit a noticeable promotion effect on the citral conversion compared with monometallic Co and Re samples (Table 4 and Figure 10). The increase of Re content has a positive influence on the amount of accessible active sites and then is beneficial to the citral conversion as well as to the cyclohexane dehydrogenation as illustrated by Figure 10(D). The FT-IR spectra of adsorbed CO over SR samples have proven the strengthening of the Co-Re interaction with the increasing of Re content (Figure 5). As anticipated, the SR-5Co-5Re/TiO$_2$ catalyst exhibits higher EOM than other SR samples when considering both Re and Co contributions (Figure 11(A)). But as highlighted by the H$_2$-TPR analysis, the core-shell structure displayed by the SR-5Co-5Re/TiO$_2$ catalyst reduces the reduction efficiency of Re species compared to other SR bimetallic catalysts exhibiting a decoration structure. This phenomenon is consistent with the EOM values related

to the lone Re contribution (Figure 11(B)) showing a superior efficiency for the SR-5Co-2Re/TiO$_2$ sample compared to SR-5Co-5Re/TiO$_2$. The enrichment of Re on the surface of catalyst, as the main contributor to citral hydrogenation, is an advantage for the production of UA since a small amount of rise in UA selectivity is observed for the SR-5Co-5Re/TiO$_2$ catalyst (Table 4).
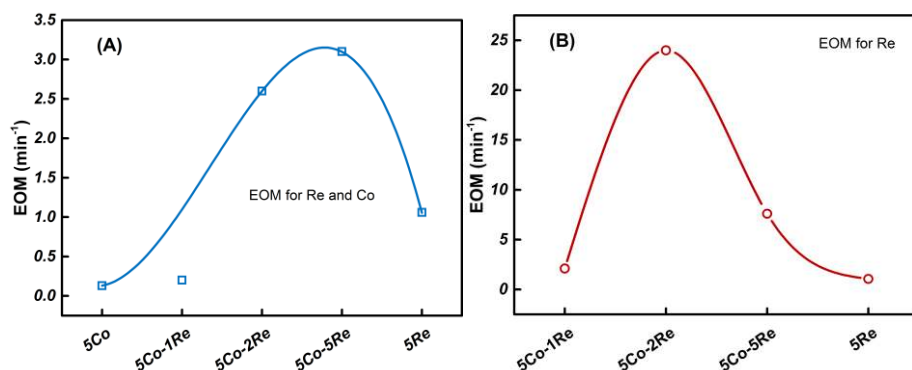

Figure 11. The efficiency of metal (EOM) for hydrogenation of citral on SR bimetallic catalysts series.

General Discussion and Conclusions

In this study, Co-Re/TiO$_2$ bimetallic catalysts were prepared by three methods: co-impregnation (CI), successive impregnation (SI) and surface redox reaction (SR). The resulting samples are distinguished from each other by their metal arrangement, which is directly related to the preparation method used. The basic difference for these samples is the contact degree between Co and Re clearly observed by TEM-EDX analysis. The CI sample presents a very limited bimetallic interaction since the particles of Re and Co are completely separated on the surface of the catalyst. The SI samples exist in a Janus-type structure because of the pre-existing metallic Co species that can contribute to the concentration of Re around Co, resulting in direct contact or at least close contact between Re and Co. Decoration/Core-shell structures are observed for SR samples due to redox reaction between Co^0 atoms of the pre-reduced Co parent catalyst and Re^{7+} ions of the modifier precursor salt. Thus, the degree of contact between the two metals gradually increases in the following order: CI sample < SI samples < SR samples. Concerning the hydrogenation of citral, SR and SI samples show higher activity than CI sample and a noticeable synergetic effect compared to Co and Re monometallic catalysts. This implies that the presence of Co-Re interaction plays a predominant role in citral transformation. In addition, the bimetallic interaction allows to increase the reduction efficiency of Re precursors (as revealed by H$_2$-TPR analysis), which is beneficial for the hydrogenation reaction according to DOS calculation. Moreover, this bimetallic interaction in the SR and SI catalysts results in an electronic transfer from Re to Co, as highlighted by *in situ* CO-FTIR analysis, which is beneficial for the adsorption of electron rich oxygen of aldehyde functions and thus beneficial for the selective hydrogenation of citral. The *in situ* CO-FTIR also proves that this electron transfer between Co and Re is more significant on SR samples than on SI ones, in agreement

with the higher degree of metal interaction for SR catalysts. Furthermore, based on H_2-TPD results, Co-Re bimetallic catalysts prepared by SI and SR methods possess more prominent hydrogen adsorption ability per mole of metal (APM) than monometallic and CI catalysts. It should also be noted that for similar metal contents, the APM of SR-5Co-2Re (1.9) is slightly higher than that of SI-4Co-1Re (1.7).

Finally, although SR samples have more significant degree of contact between the two metals and greater bimetallic interaction than SI samples, quite similar performances in citral hydrogenation are observed on both catalysts series. For example, the citral conversion (at 30 min) is 72.0 % for SI-4Co-1Re/TiO$_2$ and 77.8 % for SR-5Co-2Re/TiO$_2$, and the max yield of UA is around 44.0 % for both of them. Moreover, once Co-Re interaction has formed, it seems that excessive contact degree is unnecessary for citral hydrogenation. In fact, an excessive contact degree such as in SR-5Co-5Re/TiO$_2$ catalyst limits the reduction efficiency of Re due to the lack of directly accessible Co atoms, and then leads to a limited EOM (efficiency of metal) of Re during citral hydrogenation. Likewise, according to the H_2-TPR analysis, the SI-4Co-5Re sample exhibits lower reduction efficiency than other SI catalysts due to an aggregation of Re particles, which results in a decrease in EOM of Re. This undesirable effect of an excessive Re loading on the SI and SR series is also highlighted by H_2-TPD results, which show that the APM is compromised for the bimetallic catalysts displaying the higher Re contents.

Experimental Section

Catalysts preparation.

All the catalysts were prepared by using TiO$_2$ (from Alfa Aesar) as support, and CoCl$_2$ and NH$_4$ReO$_4$ (Alfa Aesar) as precursor salts.

Monometallic catalysts

The monometallic catalysts were prepared by impregnation in excess of solution of CoCl$_2$ or NH$_4$ReO$_4$ on TiO$_2$. The impregnated support was then dried at 90 °C for 24 h and reduced in H_2 at 500 °C for 2 h (2 °C min^{-1} heating rate). These Co or Re monometallic catalysts are referred as 5Co /TiO$_2$ or 5Re/TiO$_2$ (with 5 wt.% as expected weight metal loading).

Bimetallic catalysts

Firstly, a series of Co-Re catalysts was prepared by successive impregnation (SI) method. The NH$_4$ReO$_4$ salt was impregnated with various concentrations on monometallic 4Co/TiO$_2$. The catalysts were then dried at 90 °C for 24 h. Finally, they were reduced in H_2 at 500 °C for 2 h (2 °C min^{-1} heating rate). These Co-Re bimetallic catalysts are referred as SI-4Co-YRe/TiO$_2$ (Y represents the Re expected weight loading). A Co-Re bimetallic sample was also prepared by co-impregnation (CI) method. In this case, both CoCl$_2$ and NH$_4$ReO$_4$ precursor salts were impregnated simultaneously on TiO$_2$, and subsequent

steps were the same as described above. The corresponding catalyst is referred as Cl-4Co-1Re/TiO$_2$ (4 wt.% and 1 wt.% being the respective expected weight metal loadings).

Another series of bimetallic catalysts was also prepared by a surface redox (SR) method. This method consists of a direct surface redox reaction between the Re precursor salt and Co particles of the parent monometallic catalyst. The parent 5Co/TiO$_2$ sample was placed into a fixed-bed reactor and re-activated at 500 °C under H$_2$. Then, the NH$_4$ReO$_4$ aqueous solution (acidified to pH 1 with HCl), previously degassed under nitrogen flow, was poured onto the Co/TiO$_2$ catalyst. After 1 h reaction time under N$_2$ bubbling at room temperature, the solution was filtered out and the catalyst was dried overnight at 100 °C. Finally, the bimetallic catalysts were reduced under H$_2$ flow at 500 °C for 2 h (2 °C min^{-1} heating rate). These Co-Re bimetallic catalysts are referred as SR-5Co-YRe/TiO$_2$ (Y represents the Re expected weight metal loadings).

Catalysts characterization.

The metallic loadings of monometallic and bimetallic catalysts were analyzed by inductively coupled plasma optical emission spectroscopy (ICP-OES) equipment (Perkin Elmer Optima 2000 DV) after dissolution of the solid samples.

Powder X-ray diffraction (XRD) was used to probe metal interaction in the bimetallic catalysts and to provide information regarding crystal phases. Powder diffraction was performed on a Bruker D5005 X-ray diffractometer with a Co$K\alpha$ radiation source (λ = 1.54178 Å) and a scan speed of 0.1 ° min^{-1}.

Temperature-programmed reduction (TPR) analyses were performed on an AutoChem 2910 instrument (Micromeritics, USA) equipped with a thermal conductivity detector (TCD). The procedure for TPR analysis was as followed: the sample was heated in 10 % H$_2$/Ar at a flow rate of 30 mL min^{-1} from room temperature to 700 °C with a temperature ramping rate of 5 °C min^{-1}, and then maintained at 700 °C for 30 min.

Temperature-programmed desorption (TPD) was carried out on AutoChem 2910 instrument (Quantachrome, USA). The samples were loaded into a fritted quartz tube, pretreated at 500 °C for 120 min under 10 % H$_2$/Ar atmosphere and afterwards cooled down to 50 °C under N$_2$ atmosphere. H$_2$ adsorption was performed at 50 °C in 10 % H$_2$/Ar mixture with a flow rate of 100 mL. After H$_2$ adsorption, the samples were purged with N$_2$ for 90 min to remove physical adsorbed species. The H$_2$ desorption was then conducted under N$_2$ atmosphere with a temperature ramp of 5 °C min^{-1} from 50 to 800 °C.

The Fourier transform infrared (FT-IR) spectra of CO adsorbed over Co-Re catalysts were collected on a Bruker EQUINOX55 spectrometer. The sample was pressed into a self-supporting disk and placed in an IR cell attached to a closed glass-circulation system. Prior to CO adsorption, the sample disk was *in*

situ pre-treated at 350 °C for 2 h under H_2 and then cooled down to 30 °C. After evacuation of hydrogen by vacuum pump, the sample disk was exposed to CO for 30 min. The IR spectrum of the chemisorbed CO was recorded after physically adsorbed CO was evacuated.

Experiments of temperature programmed desorption of ammonia (NH_3-TPD) were performed on samples outgassed in He at 200 °C for 1 h, and then saturated at 50 °C in a 5.62 % NH_3/He stream (30 mL min^{-1}) for 1 h. After removing most weakly physisorbed NH_3 by flowing He (30 mL min^{-1}), the chemisorbed NH_3 quantity was analyzed with TCD detector by heating at 10 °C min^{-1} up to 800 °C and by maintaining this temperature for 30 min under the same flow of He.

Transmission electron microscopy (TEM) images were performed on a FEI Technai F20 electron microscope. The elemental mapping was achieved with energy dispersive X-ray spectroscopy (EDX) using a DX4 analyzer system The reduced catalysts were ultrasonically dispersed in ethanol and the suspension was brought onto a copper grid with carbon film. The average diameters were calculated by measuring over 100 particles from various TEM images.

The model reaction of cyclohexane dehydrogenation was performed in a fixed-bed reactor at atmospheric pressure. A mass of 80 mg of catalyst was reactivated by reduction at 500 °C for 2 h and the temperature was decreased to 300 °C to perform the reaction. Cyclohexane was injected using a calibrated motor-driven syringe (0.03 mL min^{-1}) in a hydrogen flow (100 mL min^{-1}). Cyclohexane and the products were analyzed every 10 min by GC.

Citral hydrogenation.

The hydrogenation of citral was carried out in a 250 mL autoclave with a magnetic stirrer and temperature controller unit. The catalysts (400 mg) were previously treated with H_2 for 2 h at 500 °C. After reduction, the catalysts were immersed in 90 mL of isopropanol used as solvent and transferred *in situ* into the autoclave under the protection of N_2 atmosphere by using a glove box. The batch reactor was purged first with N_2 and then with H_2 prior to raise the temperature to 70 °C. Then, a mixture of 3 mL citral and 10 mL of isopropanol was loaded into the reactor through a cylinder under 75 bar H_2 pressure. Zero time was taken at this moment. During the catalytic test, the reaction was performed under constant pressure by using a pressure control system. At different reaction times, liquid samples were manually collected and analyzed by gas chromatograph to determine the conversion and selectivity values. The efficiency of metal (EOM, with metal corresponding to Co and Re, or only Re) was calculated at citral isoconversion (20 %) using the following equation:

$$(6)\ EOM = \frac{\text{transformed citral (mol)}}{\text{reaction time (min) × metal content (mol)}}$$

Acknowledgements

[1] E. Bailón-García, F. Carrasco-Marín, A. F. Pérez-Cadenas, F. J. Maldonado-Hódar, *Appl. Catal., A* **2016**, 512, 63-73.

[2] a) P. Meric, K. Yu, A. Kong, S. Tsang, *J. Catal.* **2006**, 237, 330-336; b) U. K. Singh, M. A. Vannice, *J. Catal.* **2001**, 199, 73-84; c) M. S. Ide, B. Hao, M. Neurock, R. J. Davis, *ACS Catal.* **2012**, 2, 671-683.

[3] a) A. Vicente, G. Lafaye, C. Especel, P. Marécot, C. T. Williams, *J. Catal.* **2011**, 283, 133-142; b) T. Ekou, A. Vicente, G. Lafaye, C. Especel, P. Marecot, *Appl. Catal., A* **2006**, 314, 64-72; c) C. Especel, D. Duprez, F. Epron, *C. R. Chim.* **2014**, 17, 790-800.

[4] a) D. D. Falcone, J. H. Hack, R. J. Davis, *ChemCatChem* **2016**, 8, 1074-1083; b) Z. Wei, A. M. Karim, Y. Li, D. L. King, Y. Wang, *J. Catal.* **2015**, 322, 49-59; c) X. Di, C. Li, B. Zhang, J. Qi, W. Li, D. Su, C. Liang, *Ind. Eng. Chem. Res.* **2017**, 56, 4672-4683; d) X. Di, C. Li, G. Lafaye, C. Especel, F. Epron, C. Liang, *Catal Sci Technol* **2017**, 7, 5212-5223.

[5] a) T. N. Phaahlamohlaka, D. O. Kumi, M. W. Dlamini, R. Forbes, L. L. Jewell, D. G. Billing, N. J. Coville, *ACS Catal.* **2017**, 7, 1568-1578; b) S. K. Beaumont, S. Alayoglu, C. Specht, N. Kruse, G. A. Somorjai, *Nano Lett.* **2014**, 14, 4792-4796; c) M. Hosseini, T. Barakat, R. Cousin, A. Aboukaïs, B. L. Su, G. De Weireld, S. Siffert, *Appl. Catal., B* **2012**, 111-112, 218-224; d) D. Nabaho, J. W. Niemantsverdriet, M. Claeys, E. van Steen, *Catal. Today* **2016**, 261, 17-27; e) S. Alayoglu, B. Eichhorn, *J. Am. Chem. Soc.* **2008**, 130, 17479-17486.

[6] a) R. Prins, *Chem. Rev.* **2012**, 112, 2714-2738; b) V. V. Rozanov, O. V. Krylov, *Russ. Chem. Rev.* **1997**, 66, 107-119.

[7] a) B. K. Ly, B. Tapin, M. Aouine, P. Delichere, F. Epron, C. Pinel, C. Especel, M. Besson, *ChemCatChem* **2015**, 7, 2161-2178; b) L. Corbel-Demailly, B. K. Ly, D. P. Minh, B. Tapin, C. Especel, F. Epron, A. Cabiac, E. Guillon, M. Besson, C. Pinel, *ChemSusChem* **2013**, 6, 2388-2395.

[8] a) S. Storsater, O. Borg, E. Blekkan, A. Holmen, *J. Catal.* **2005**, 231, 405-419; b) A. M. Hilmen, D. Schanke, K. F. Hanssen, A. Holmen, *Appl. Catal., A* **1999**, 186, 169-188.

[9] a) L. Zhang, L. Wan, Y. Ma, Y. Chen, Y. Zhou, Y. Tang, T. Lu, *Appl. Catal., B* **2013**, 138-139, 229-235; b) J. X. Wang, C. Ma, Y. Choi, D. Su, Y. Zhu, P. Liu, R. Si, M. B. Vukmirovic, Y. Zhang, R. R. Adzic, *J. Am. Chem. Soc.* **2011**, 133, 13551-13557.

[10] a) H. Iida, A. Igarashi, *Appl. Catal., A* **2006**, 303, 48-55; b) C. Bolivar, H. Charcosset, R. Frety, M. Primet, L. Tournayan, C. Betizeau, G. Leclercq, R. Maurel, *J. Catal.* **1976**, 45, 163-178.

[11] a) Y. Sato, Y. Soma, T. Miyao, S. Naito, *Appl. Catal., A* **2006**, 304, 78-85; b) W. Daniell, *J. Mol. Catal. A: Chem.* **2003**, 204-205, 519-526.

[12] a) W. Rachmady, M. A. Vannice, *J. Catal.* **2000**, 192, 322-334; b) D. S. Park, D. Yun, T. Y. Kim, J. Baek, Y. S. Yun, J. Yi, *ChemSusChem* **2013**, 6, 2281-2289.

[13] a) Y. Ma, X. Wu, G. Zhang, *Appl. Catal., B* **2017**, 205, 262-270; b) O. R. Inderwildi, S. J. Jenkins, D. A. King, *Surf. Sci.* **2007**, 601, 103-108.

Supported Co-Re bimetallic catalysts with different structures as efficient catalysts for hydrogenation of citral

Xin Di [a], [b], Gwendoline Lafaye *[b], Catherine Especel [b], Florence Epron [b], Ji Qi [a], Chuang

Li [a], Changhai Liang *[a]

[a] Laboratory of Advanced Materials and Catalytic Engineering, Dalian University of

Technology, P.R. China

[b] Institut de Chimie des Milieux & Matériaux de Poitiers (IC2MP), Université de Poitiers, 4 rue
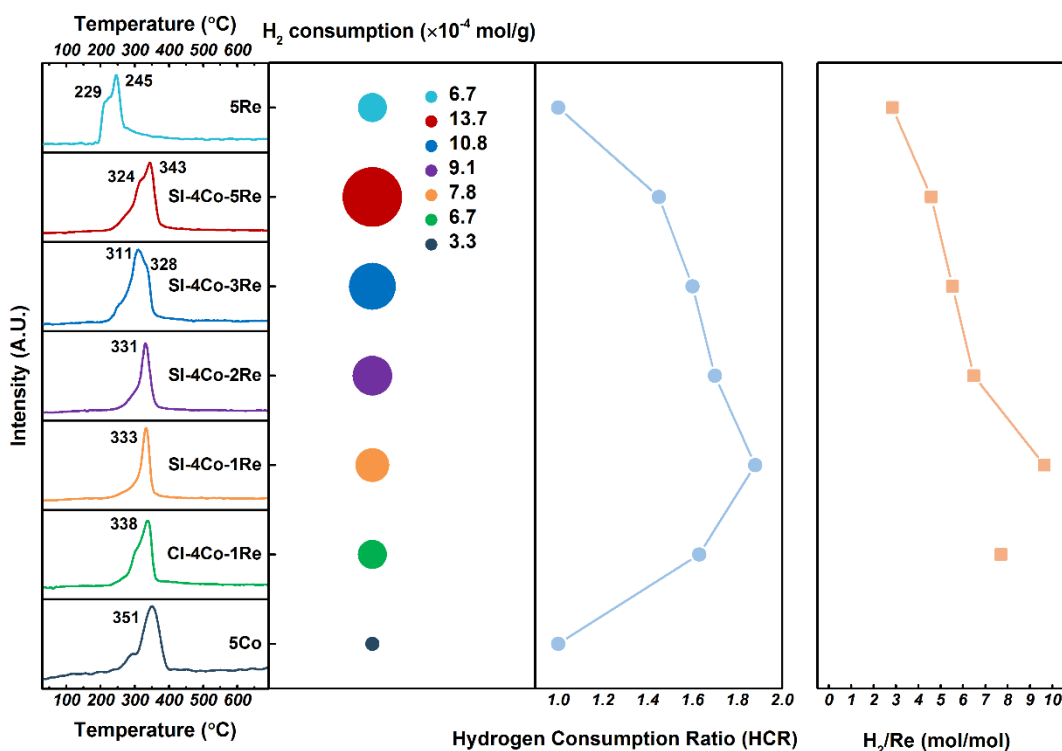Michel Brunet, 86073 Potiers Cedex 9, France

Figure S1. H_2-TPR results of SI-4Co-XRe/TiO$_2$, CI-4Co-1Re/TiO$_2$, 5Co/TiO$_2$ and 5Re/TiO$_2$.

The hydrogen consumption ratio (HCR) and molar H_2/Re ratio were calculated according to the following respective equations:

(1) Hydrogenation consumption ratio (HCR) $= \dfrac{\text{Actual hydrogen consumption (mol/g}_{\text{catalyst}})}{\text{Expected hydrogen consumption (mol/g}_{\text{catalyst}})}$

(2) Expected hydrogen consumption (mol/g$_{\text{catalyst}}$)=

$\dfrac{\text{Co loading of Co-Re/TiO}_2}{\text{Co loading of Co/TiO}_2} \times (3.3 \times 10^{-4}) + \dfrac{\text{Re loading of Co-Re/TiO}_2}{\text{Re loading of Re/TiO}_2} \times (6.7 \times 10^{-4})$

(3) H_2/Re $= \dfrac{\text{Actual hydrogen consumption} - \dfrac{\text{Co loading of Co-Re/TiO}_2}{\text{Co loading of Co/TiO}_2} \times (3.3 \times 10^{-4})}{\text{Molar amount of Re/g}_{\text{catalyst}}}$

In equations (2) and (3), the 3.3×10^{-4} and 6.7×10^{-4} values correspond respectively to the H_2 consumption (mol/g$_{\text{catalyst}}$) of pre-oxidized Co/TiO$_2$ and Re/ TiO$_2$ catalysts determined by TPR. The hydrogen consumption ratio (HCR) for SI bimetallic catalysts is significantly higher than that exhibited by monometallic Co and Re catalysts, which suggests that contact between Re

and Co species was established modifying their reduction properties. There is clearly a strong effect of Co on the reduction of ReOx. The H_2/Re ratio is higher for the SI bimetallic catalysts compared to the Re monometallic sample and decreases when the Re content increases. This trend is consistent with the HCR values, indicating the presence of aggregated Re particles that reduces the reduction efficiency. Furthermore, a comparison of CI-4Co-1Re/TiO$_2$ and SI-4Co-1Re/TiO$_2$ catalysts evidences significantly lower HCR and H_2/Re ratios for the CI sample, which means weaker Co-Re interaction in this case. It is noteworthy that the HCR and H_2/Re values of CI-4Co-1Re are higher than those of monometallic samples. Co-Re interaction in CI sample could be slightly strengthened after oxygen treatment applied before the TPR analysis.
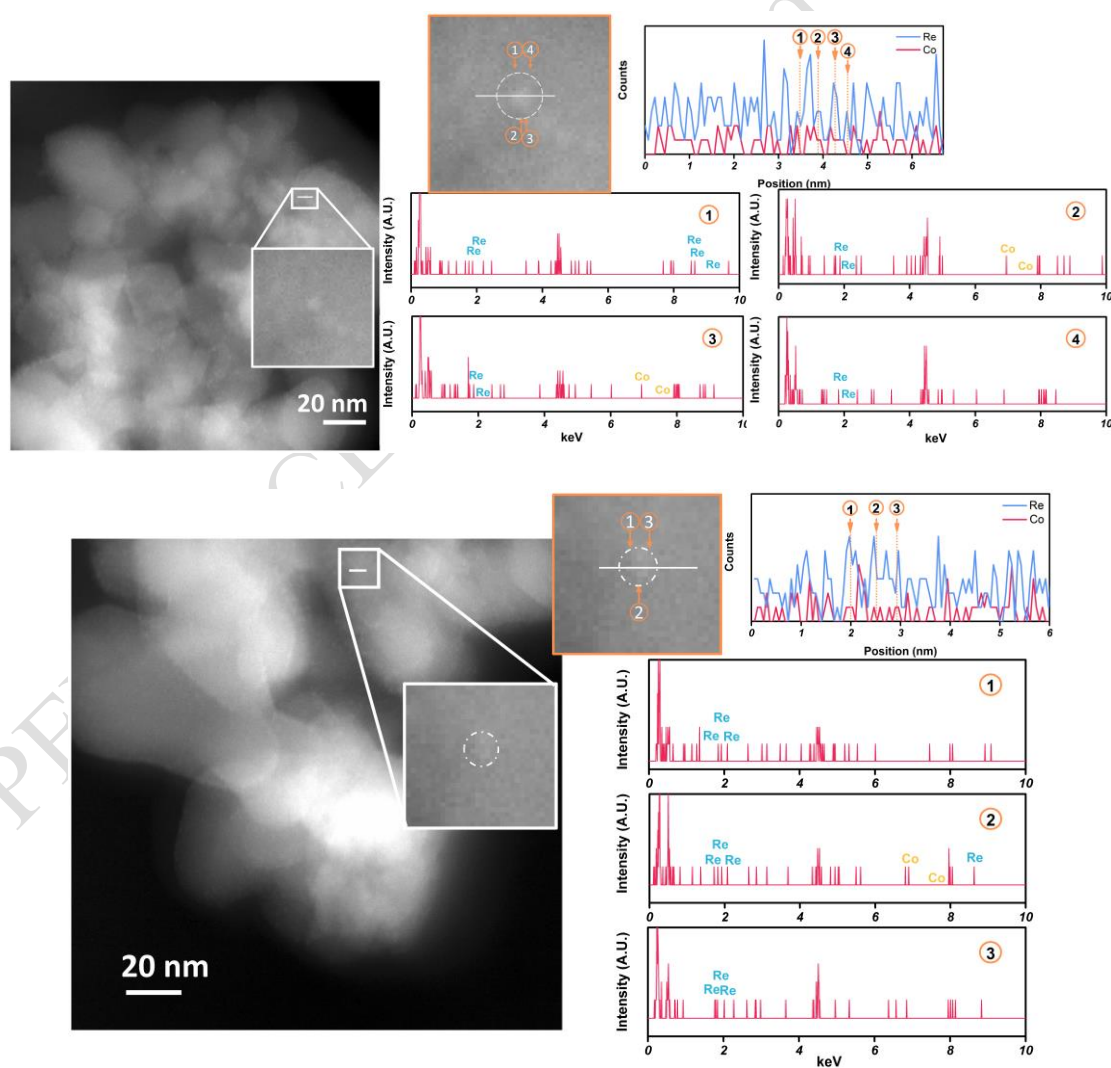

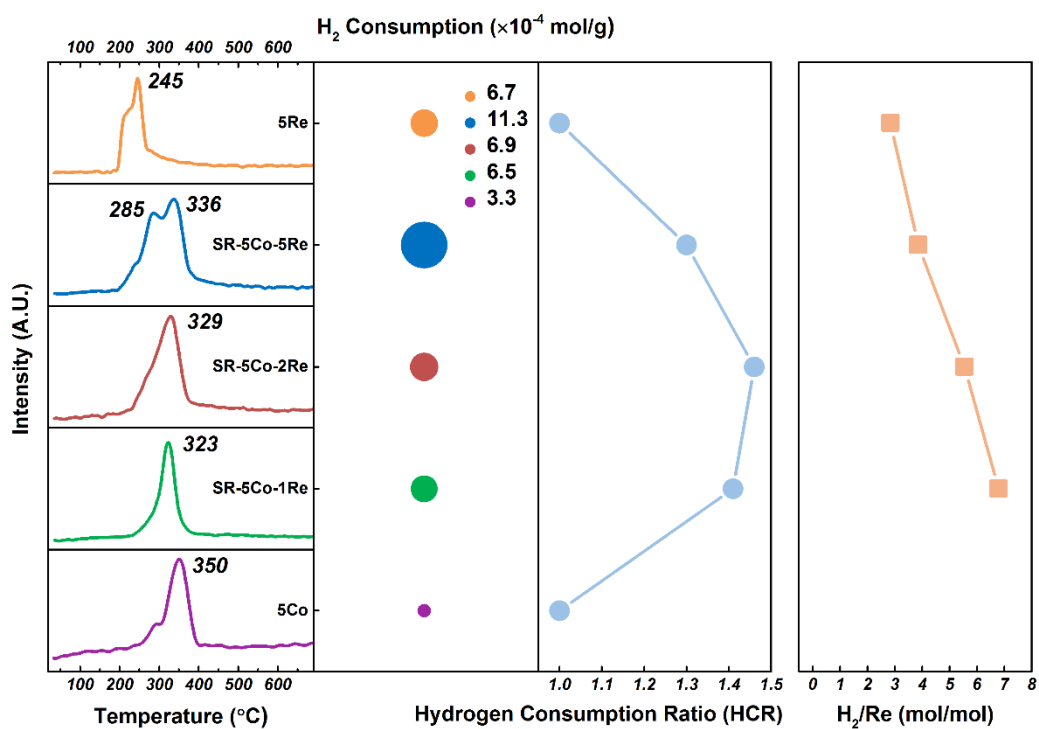Figure S2. HAADF-STEM, linearly scanning and associated EDX of SR-5Co-5Re/TiO$_2$.

Figure S3. H_2-TPR results of SR-5Co-XRe/TiO$_2$ catalysts.